JOURNAL OF APPLIED ELECTROCHEMISTRY **28** (1998) 311–319

Dynamic modelling of gas hold-up in different electrolyte systems*‡

H. KELLERMANN, K. JÜTTNER, G. KREYSA

Karl-Winnacker-Institut der DECHEMA e.V., Postfach 15 01 04, D-60061 Frankfurt am Main, Germany

Received 21 January 1997; revised 30 June 1997

In measurements of gas hold-up of oxygen and hydrogen as a function of the gas flow rate it was found that the gas hold-up $\varepsilon(u_g^0)$ depends on the type of electrolyte and its concentrations as well as on the type of gas. Using an ultrasonic Doppler velocimeter, bubble rise velocities were investigated. It was observed that the single bubble rise velocity in electrolyte solutions depended strongly on the concentration. A model, developed to take into account the impediment to coalescence by electrolytes, was used to evaluate the dependence of gas hold-up on electrolyte concentration. An almost linear correlation between the system specific parameter, ε_{max}, of this model and the ionic strength was found. However, this correlation is not too accurate and can only be seen as a rough approximation. Experimental results indicate that another mechanism is responsible for the dependence of the gas hold-up on electrolyte concentration. Thus, a new model was derived, which incorporated results of measurements of bubble rise velocities. This model was also applied to describe the gas hold-up in different electrolyte solutions as a function of gas flow rate. It also includes a system-specific parameter. The dependence of this parameter on the concentration of electrolytes was found to be in accordance with current theories on the bubble coalescence.

Keywords: *gas hold-up*, *oxygen*, *hydrogen*, *rise velocity*, *bubbles*, *electrolytes*

List of symbols

A_{bc}	cross-sectional area of the bubble column (m^2)
A_{gs}	cross-sectional area of the gas sparger (m^2)
$c_{b,i}$	number of bubbles with diameter $d_{b,i}$ per unit volume (m^{-3})
$d_{b,i}, d_b$	bubble diameter (m)
$\bar{d}_b$	mean bubble diameter (m)
ε	gas hold-up
ε_{max}	maximum gas hold-up
k	coalescence impact parameter (m)
l	length of coalescence zone (mm)
N	number of bubble classes
$\nu_{ih}, \nu_{jh}, \nu_{kh}$	'stoichiometric factors' of the coalescence 'reaction'
u_b	bubble rise velocity (cm s^{-1})
u_g^0, u_l^0	superficial gas (liquid) velocity (cm s^{-1})
u_s	single bubble rise velocity (cm s^{-1})
$u_{s,cbm}$	single bubble rise velocity from fits of the coalescence barrier model (cm s^{-1})
$\overline{u}_s$	mean single bubble rise velocity (cm s^{-1})
u_{sw}	rise velocity of a bubble swarm (cm s^{-1})
v_c	circulation velocity of eddy above the gas sparger (cm s^{-1})
V	total volume of the two phase system (m^3)
z	vertical distance to gas sparger (mm)

1. Introduction

In many electrochemical processes, such as the alkali chloride and water electrolysis, gas evolution at electrodes determines the effective conductivity of the electrolyte. To estimate the *IR*-drop in an electrochemical cell knowledge of the gas hold-up is of paramount importance [1–5]. Many investigations have dealt with the dependence of the gas hold-up, ε, on gas flow rate u_g^0 in electrolyte solutions [2, 3, 5–18]. A number of different models have been derived to describe the dependence of ε on u_g^0 [3, 5–8, 10, 13, 14], which do not take into account the coalescence of bubbles. On the other hand the dynamics of the coalescence process have been investigated by other authors [19–23]. Most investigations on the influence of the coalescence behaviour on the gas hold-up and the interfacial area, depending on the concentration and the type of electrolyte, either use empirical approaches to obtain correlations between the gas hold-up and physico-chemical properties in the different electrolyte solutions [10] or interpret their data only qualitatively [12, 15, 24]. In other studies the effect of coalescence on the gas hold-up is considered as a consequence of turbulent flow [13, 14]. But coalescence also affects gas hold-up in homogenous bubble

* This paper was presented at the Fourth European Symposium on Electrochemical Engineering, Prague, 28–30 August 1996.
‡ Dedicated to Prof. Dr Ulrich Hoffmann on the occasion of his 60th birthday.

0021-891X

flow [3, 5, 19]. Previous investigations indicate that a coalescence barrier must exist in order to explain the maximum gas hold-up observed in different systems. This maximum gas hold-up was found to depend not only on the type of electrolyte, but also on the nature of the gas [3, 5]. A defined correlation between the gas hold-up maximum and other system specific parameters has not been determined to date. The coalescence barrier may be explained by the existence of repulsive forces arising from an electric excess charge at the bubble surface as found by Fukui and Yuu [25], Brandon *et al.* [26] and Kelsall *et al.* [27] from electrophoretic measurements on single bubbles.

This work aims to gain detailed information on the gas hold-up in different electrolytes containing Li^+, Na^+, K^+ or H^+ as cations and Cl^-, SO_4^{2-}, OH^- as anions. To study the gas hold-up of oxygen and hydrogen under well defined conditions over a wide range of gas flow rates, systematic measurements were carried out using a bubble column at laboratory scale.

2. Fundamental theory

For a comprehensive representation of theoretical models it is useful to provide a brief definition of the most important quantities:

(i) Gas hold-up, ε, is the fraction of volume occupied by bubbles, $\varepsilon = N_b V_b / V$.
(ii) Superficial gas velocity, u_g^0, is defined as $u_g^0 = \dot{V}_{gas}/A_{bc}$
(iii) Superficial liquid velocity, u_l^0, is defined as $u_l^0 = \dot{V}_{liquid}/A_{bc}$.
(iv) Single bubble rise velocity, u_s, is the velocity achieved by a single bubble in an infinite liquid. This velocity is sometimes called the slip velocity because it is the relative velocity between a gas bubble and the quiescent liquid.
(v) Rise velocity, u_{sw}, of a swarm of bubbles in a quiescent liquid is the velocity a swarm of bubbles will have when the gas supply is shut off and the liquid above is at rest.
(vi) Rise velocity, u_b, is the actual vertical velocity of a gas bubble in any gas–liquid system.

An axisymmetric volume, V, will be considered as a frame of reference. This volume includes N_b bubbles, each occupying a volume V_b. The control volume is bounded by two horizontal surfaces with surface area A_{bc}, and height V/A_{bc}. Gas bubbles rise perpendicular to the surface with velocity u_b.

Within the time period dt a number of $N_{b,out} = N_b(A_{bc}/V)u_b\,dt$ bubbles will leave the volume V. Hence, the volume output is given by

$$\dot{V}_{g,out} = \frac{N_b V_b A_{bc} u_b}{V} \tag{1}$$

where $N_b V_b / V$ is the gas hold-up ε. The gas volume entering the lower boundary of the control volume, is

$$\dot{V}_{g,in} = u_g^0 A_{bc} \tag{2}$$

For steady state operation the input and the output of gas volume are equal ($\dot{V}_{g,in} = \dot{V}_{g,out}$). Hence,

$$u_g^0 = u_b \varepsilon \;\Leftrightarrow\; \varepsilon = u_g^0/u_b \tag{3}$$

Nicklin [6] showed that

$$u_b = u_g^0 + u_l^0 + u_{sw} \tag{4}$$

where the bubble swarm velocity u_{sw} depends on the gas holdup ε. Several equations have been proposed to represent the dependence of u_{sw} on gas hold-up ε. Marrucci [28] derived the expression

$$u_{sw} = \frac{u_s(1-\varepsilon)^2}{1-\varepsilon^{5/3}} \tag{5}$$

by evaluating the energy dissipation of an irrotational flow around a spherical bubble.

Lockett and Kirkpatrick [8] adapted an empirical approach,

$$u_{sw} = u_s(1-\varepsilon)^{2.39}(1+2.55\,\varepsilon^3) \tag{6}$$

which fitted their experimental data better than Equation 5 or other approaches. Considering their experimental setup and Marrucci's calculations it can be clearly seen that a normalized form of Equation 5 should be used to compare the measured velocities in their experiments, rather than the original form of Equation 5. Equation 5, with a normalized gas hold-up $\varepsilon/0.74$ instead of ε, provides velocities close to those obtained from Equation 6 up to a gas hold-up of about 0.4. The preferred function $u_{sw} = f(\varepsilon)$ is the theoretical one of Marrucci, which also provides a suitable approach for normalization with the maximum gas hold-up, ε_{max}, as proposed by Kreysa and Kuhn [3, 5].

Substitution of u_b in Equation 3 by Equation 4 and using Equation 5 for the expression of u_{sw} leads to:

$$\varepsilon = \frac{u_g^0}{u_g^0 + u_l^0 + u_s\frac{(1-\varepsilon)^2}{1-\varepsilon^{5/3}}} \tag{7}$$

This implicit equation for the function $\varepsilon = f(u_g^0)$ can be solved by standard numerical algorithms, for example, the Euler procedure.

3. Experimental details

To confirm predictions of the coalescence barrier model, which is described below, the gas hold-up and the rise velocity are investigated in several electrolyte solutions. Gas hold-up measurements were carried out in a glass bubble column of 38 mm inside diameter and 60 cm height. The gas bubbles were generated using a glass frit of 10–14 μm pore size. The gas hold-up ε was determined as a function of the superficial gas velocity, u_g^0, measuring the hydrostatic pressure drop, which is a widely used method for gas hold-up measurements [29–32]. These measurements of the gas hold-up were compared to direct measurement of the height of the two phase system. The results of both methods agreed within 5% at homogeneous bubble flow and 10% in the turbulent flow regime. The accuracy of gas hold-up measurements by hydrostatic pressure drop is $\Delta\varepsilon = 0.007$; the accuracy of the direct method is $\Delta\varepsilon = 0.02$.

Additionally the bubble rise velocity was measured by an ultrasonic Doppler probe technique [33] (Fig. 1). The ultrasonic Doppler measurement device consists of a probe that sends and receives ultrasonic pulses, an electrical signal processing unit, that generates sending signals and collects and transforms frequency information from received signals into velocity data, and a personal computer, which controls the processing unit. For a time interval of 3 μs the ultrasonic probe sends a pulse with a frequency of 4 MHz. This pulse is reflected by a bubble. The signal received by the probe has a frequency, which is shifted by $\Delta f = 2u_b f_s/c_s$. Signals are analysed by fast Fourier transformation and stored as frequency distribution at the signal processing unit. A velocity distribution is computed by the measurement control program running at the personal computer. With this apparatus velocities can be measured with an accuracy of 1 cm s^{-1} [33]. The ultrasonic probe was tested by measuring the rise velocity of bubbles having a diameter of 4.6 to 5.2 mm in 2 M NaCl. The bubbles were generated by a capillary at a constant gas flow rate, which was controlled by a calibrated gas flow controller. The number of bubbles generated was counted for 20 s.

From bubble frequency and gas flow rate the bubble volume and the corresponding diameter was derived. The mean values of bubble rise velocity measured with the ultrasonic probe were 22.9 to 23.5 cm s^{-1}, which is in good agreement with predictions from theory [37] of 23.0 to 23.2 cm s^{-1}. The rise velocities measured by the ultrasonic probe technique were found to agree within 10 to 15% with u_b-values derived by gas hold-up data by $u_b = u_g^0/\varepsilon$ if the gas flow rate was $0.1\,\mathrm{cm\,s^{-1}} < u_g^0 < 1.0\,\mathrm{cm\,s^{-1}}$. The deviations in that range of gas flow rates may be explained by errors in measuring the gas hold-up and the rise velocities (see above). At higher gas flow rates the rise velocities measured by the ultrasonic technique are significantly higher than the velocities derived from gas hold-up data, if they were measured at the centre of the bubble column. The velocities measured beneath the rim of the column are lower than velocities from gas hold-up data. This points to a radial distribution of bubble velocities in the bubble column, as is found in tall bubble columns [34–36].

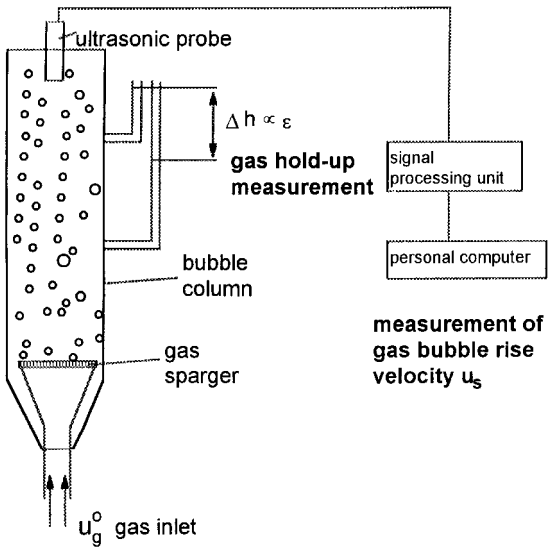

Fig. 1. Experimental setup for the gas hold-up measurements.

Table 1. Systems studied

Electrolyte	*Concentration range*/M	Gas
H_2O	–	O_2, H_2
Li_2SO_4	0.1–0.3	O_2
Na_2SO_4	0.02–1.0	O_2, H_2
K_2SO_4	0.02–0.3	O_2
NaCl	0.1–4.0	O_2
KCl	1.0–4.0	O_2
NaOH	0.01–4.0	O_2, H_2
H_2SO_4	1.0–2.0	O_2, H_2

To study the influence of the electrolyte on the gas hold-up of oxygen and hydrogen measurements were performed in different electrolyte systems over a wide range of concentrations (Table 1). To obtain reproducible results all solutions were prepared from p.a. grade chemicals (Merck AG) and deionized and distilled water. All parts of the bubble column, and all flasks containing the solutions, were cleaned with chromic acid and treated with distilled water and steam before use. The solutions were purged for one hour at a gas hold-up of oxygen or hydrogen of 10–20%. To ensure reproducibility for each value of the superficial gas velocity, u_g^0, the gas hold-up, ε was measured at least twice. Moreover, multiple independent experiments were conducted. The velocity measurements were made after the gas hold-up experiments had been carried out. Further details on the experimental procedure are given elsewhere [16].

4. Results and discussion

A typical set of gas hold-up measurements is given in Fig. 2, which shows the hold-up of O_2 as a function of superficial gas velocity u_g^0 in pure water and NaOH

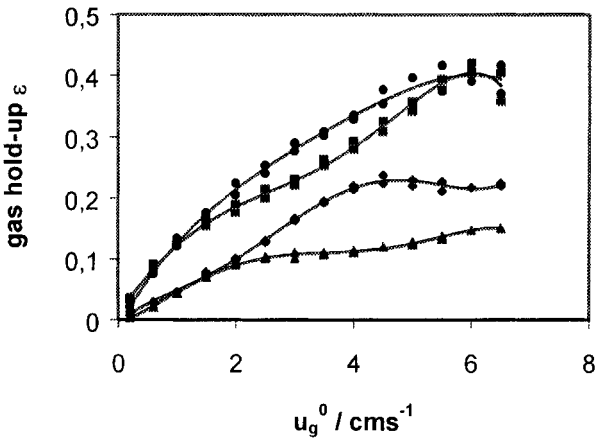

Fig. 2. Gas hold-up of O_2 as a function of the superficial gas velocity u_g^0 in pure water and NaOH solutions. 0.1 M NaOH/O_2 (●); 0.5 M NaOH/O_2 (■); 1.0 M NaOH/O_2 (◆); water/O_2 (▲).

solutions. Independent of the electrolyte concentration it is found that ε increases almost linearly with rising u_g^0 up to a limiting value. A similar behaviour has also been described by Kuhn and Kreysa [3, 5].

This limiting value, ε, shows a distinct dependence on the concentration and the type of gas [18]. In general, the maximum value of the gas hold-up, ε, increases with the electrolyte concentration. The lowest gas hold-up value is found in pure water. The same behaviour has been observed for hydrogen bubbles (Fig. 3), but the maximum values of gas hold-up are significantly higher for high concentrations. This effect is also evident in Na_2SO_4 solutions (Fig. 4).

The differences observed in the gas hold-up are probably due to the different coalescence behaviour of hydrogen and oxygen bubbles, as also found for bubbles adhering to electrodes [36].

In further experiments the bubble rise velocity was measured in order to characterize the gas sparger and to verify theoretical implications made to describe the gas hold-up. Figure 5 shows the bubble rise velocities at a very low gas flow rate ($u_g^0 = 0.001\,\mathrm{cm\,s^{-1}}$) and gas hold-up ($\varepsilon \to 0$) with different Na_2SO_4 concentrations. The rise velocity of a bubble under these conditions can be assumed to be equal to the single bubble rise velocity, u_s, of a bubble originally formed at the gas sparger without any effects of coalescence.

In Fig. 5 a drop in the rise velocity is found for increasing electrolyte concentrations at $c \approx 0.1\,\mathrm{mol\,dm^{-3}}$. For higher concentrations the decrease of bubble rise velocity with increasing concentration is in accordance with theoretical predictions for a bubble with a diameter of 0.24 mm [37]. This indicates that, for low concentrations, bubbles produced at the gas sparger coalesce even at gas flow rates as low as $u_g^0 = 0.001\,\mathrm{cm\,s^{-1}}$. In solutions with higher concentrations coalescence obviously does not affect the size and rise velocity of bubbles at these gas flow rates, so that the size of bubbles, which are directly generated at the gas sparger, can be estimated.

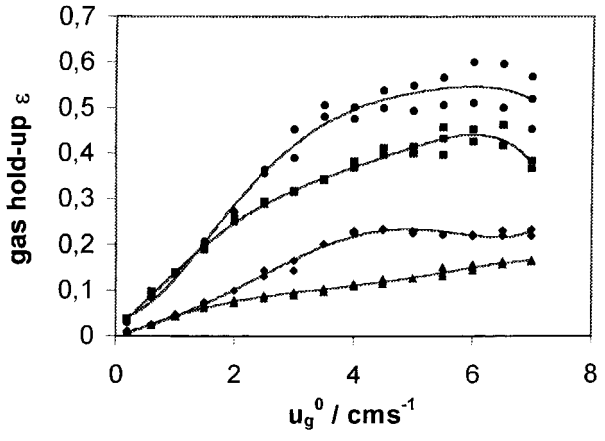

Fig. 3. Gas hold-up of H_2 as a function of the superficial gas velocity u_g^0 in pure water and NaOH solutions. 0.1 M NaOH/H_2 (●); 0.5 M NaOH/H_2 (■); 1.0 M NaOH/H_2; (◆); water/H_2 (▲).

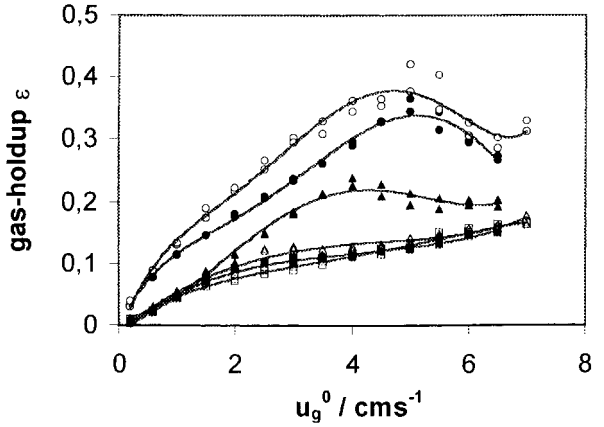

Fig. 4. Gas hold-up of O_2 and H_2 as a function of the superficial gas velocity u_g^0 in pure water and Na_2SO_4 solutions. Water/O_2 (■); water/H_2 (□); 0.02 M Na_2SO_4/O_2 (▲); 0.02 M Na_2SO_4/H_2 (△); 0.1 M Na_2SO_4/O_2 (●); 0.02 M Na_2SO_4/H_2 (○).

4.1. *Coalescence barrier model*

Conventional models based on the approach of Nicklin Equation 7 can describe the general dependence of the gas hold-up on u_g^0. However, the observed limiting values, which in the following will be denoted as ε_{max}, cannot be explained by these models. According to Equation 7, the maximum should approach the limiting value $\varepsilon_{max} = 1$. The ε_{max} values observed are significantly lower than 1. Obviously, this is due to repulsive forces which drive the bubbles apart, leading to a minimum distance, a_{min}, between the bubbles. The corresponding energetic situation is shown schematically in Fig. 6. Provided the electrical charge of bubbles, which has been measured in carefully purified dilute electrolyte solutions by Fukui and Yuu [25], Brandon *et al.* [26] and Kelsall *et al.* [27] is also present at higher electrolyte concentrations $c > 10^{-3}$ M, an electrostatic repulsive force between bubbles should exist.

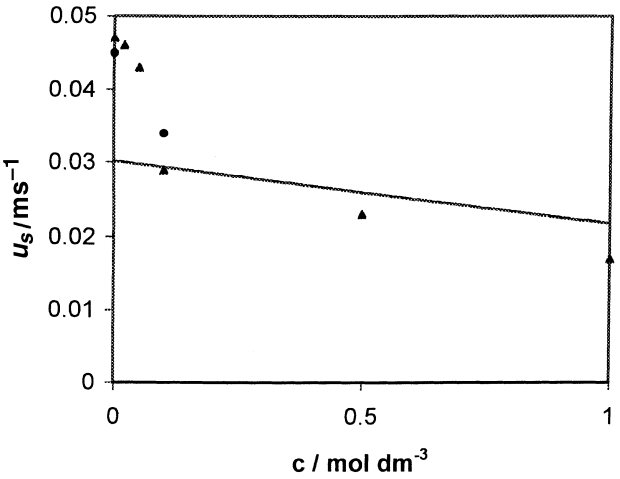

Fig. 5. Single bubble rise velocity of O_2 and H_2 bubbles as a function of the Na_2SO_4 concentration at constant $u_g^0 = 0.001\,\mathrm{cm\,s^{-1}}$. Experimental data: Na_2SO_4/O_2 (●); Na_2SO_4/H_2 (▲). Calculation of $u_s = f(c)$ for $d_b = 0.24\,\mathrm{mm}$ using an equation given by Jamialahmadi *et al.* [37] immobile gas-liquid interface (——).

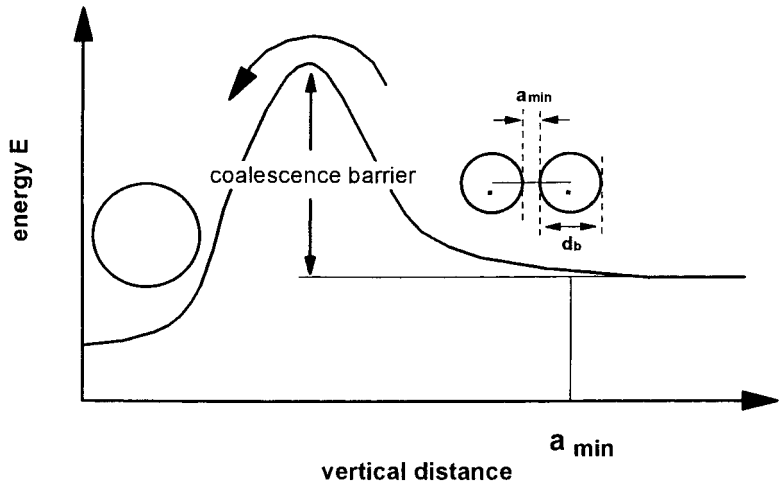

Fig. 6. Coalescence barrier model [3, 5].

Based on these considerations the coalescence barrier model proposed by Kuhn and Kreysa [3, 5] leads to the following modification of the Nicklin equation.

$$\varepsilon = \frac{\varepsilon_{max} u_g^0}{u_g^0 + u_l^0 \frac{\varepsilon_{max}-\varepsilon}{1-\varepsilon} + u_s\, \varepsilon_{max} \frac{(1-\varepsilon/\varepsilon_{max})^2}{1-(\varepsilon/\varepsilon_{max})^{5/3}}} \qquad (8)$$

where ε_{max} appears as an additional system specific parameter. As an example Fig. 7 shows experimental results and curves generated, using optimum fit parameters ε_{max} and u_s. The experimental results are well described by Equation 8. However, the values of the single bubble rise velocity $u_{s,cbm}$ evaluated from the fit, deviate significantly from the values $u_{s,exp}$, measured with the ultrasonic technique.

Figure 8 shows the dependence of the fit parameter ε_{max} for O_2 on the concentration in different electrolyte solutions. The maximum gas hold-up, ε_{max}, shows a correlation with the electrolyte concentration, c, which can be roughly approximated by a straight line $\varepsilon_{max} = a_1 c + b_1$ for 1–1-electrolytes and $\varepsilon_{max} = a_2 c + b_2$ for 1–2-electrolytes, where $b_1 \approx b_2 \approx 0.2$ and $a_2 \approx 3a_1$. This indicates that a unique linear correlation between ε_{max} and the ionic strength $I = \frac{1}{2}\sum_{\text{all ions } i} c_i z_i^2$ exists, as shown in Fig. 9. Although the fit is poor, this correlation supports the idea of the existence of repulsive electrostatic interaction between gas bubbles as the main reason for a coalescence barrier [3, 5], but the Debye-length in a 0.1 M solution of a 1–1-electrolyte is as thin as 1 nm and it is therefore not likely that an electric double layer will hinder bubbles from coalescing or even drive them apart.

Both the coalescence barrier model and the conventional models imply the existence of a unique bubble rise velocity, u_s, independent of the gas flow rate per unit area, u_g^0, neglecting coalescence of bubbles. Figure 10 shows normalized bubble rise velocity distributions of O_2 in H_2O and 0.1 M Na_2SO_4 at three different gas flow rates. These results clearly indicate that the rise velocity is not constant. In both systems the maximum of the velocity distribution shifts to higher values with increasing u_g^0. In pure water a separation of two maxima of the u_b distribution arises at $u_g^0 = 0.2\,\text{cm s}^{-1}$. Moreover, in both systems, on increasing the gas flow rate a broadening of the distribution is also evident. These experimental findings suggest that u_s depends on u_g^0 and cannot be con-

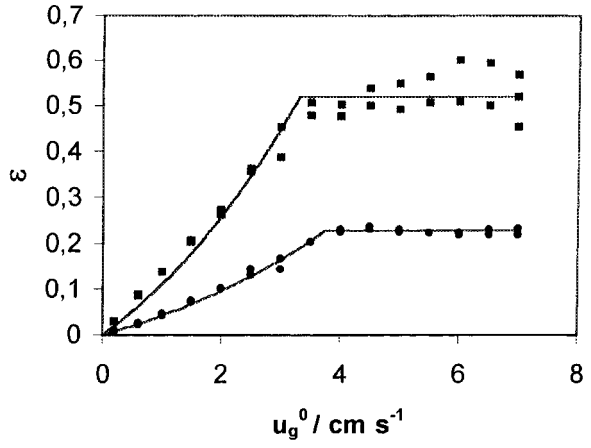

Fig. 7. Fits of experimental gas hold-up curves using the coalescence barrier model Equation (8) of Kreysa and Kuhn. System: 0.1 M NaOH/H_2 (■); fit parameter: $\varepsilon_{max} = 0.226$; $u_s = 10.6\,\text{cm s}^{-1}$; experimental value $u_{s,exp} = 3.9\,\text{cm s}^{-1}$ (ultrasonic measurements). System: 1.0 M NaOH/H_2 (●); $\varepsilon_{max} = 0.519$; $u_s = 10.6\,\text{cm s}^{-1}$; $u_{s,exp} = 2.5\,\text{cm s}^{-1}$.

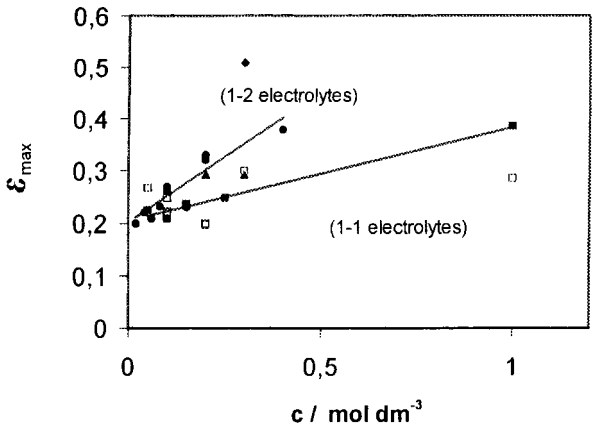

Fig. 8. Dependence of the maximum gas hold-up ε_{max} of O_2 on the electrolyte concentration c in different solutions: Li_2SO_4 (▲); Na_2SO_4 (●); K_2SO_4 (◆); NaCl (■); NaOH (□).

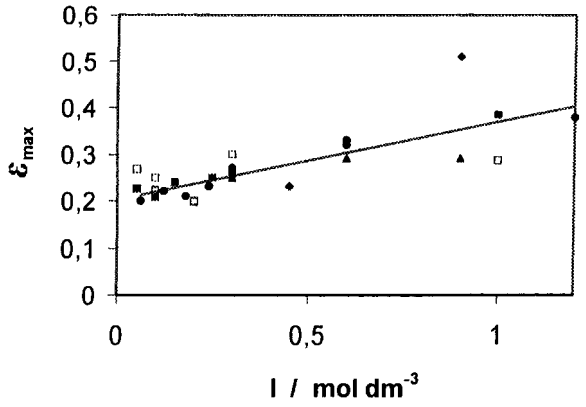

Fig. 9. Dependence of the maximum gas hold-up ε_{max} of O_2 on the ionic strength, I, in different solutions: Li_2SO_4 (▲); Na_2SO_4 (●); K_2SO_4 (◆); NaCl (■); NaOH (□).

sidered as a constant parameter in the Nicklin equation (Equation 7) or in the modified Nicklin equation (Equation 8). Evidently coalescence events are involved in the fluid dynamics of bubble flow and have to be considered in a comprehensive model.

4.2. *Coalescence zone model*

A new model which takes into account the coalescence of gas bubbles, leading to a distribution of the bubble rise velocity dependent on gas flow rate u_g^0, has been derived (Fig. 11). From ultrasonic measurements (Fig. 12) it can be seen that coalescence mainly occurs within a small zone above the gas sparger [11, 17, 19]. In this region a higher gas bubble velocity is observed due to the existence of a liquid circulation flow which promotes the coalescence of bubbles. Above the coalescence zone a homogeneous flow regime prevails (Fig. 11).

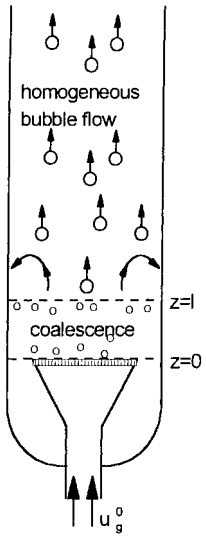

Fig. 11. Scheme of coalescence and homogenous bubble flow zones in the bubble column and liquid circulation flow.

In the zone with homogeneous bubble flow a mathematical description of the gas hold-up behaviour is provided by the conventional Nicklin approach

$$\varepsilon = \frac{u_g^0}{u_g^0 + u_l^0 + \overline{u}_s\left(\frac{(1-\varepsilon^2)}{1-\varepsilon^{5/3}}\right)} \tag{9}$$

where $\overline{u}_s$ denotes the mean bubble rise velocity. This term depends specifically on the interaction of bubbles in the coalescence zone. Modelling of the coalescence events is based on the kinetic impact theory [14, 17, 21]. The mean bubble rise velocity is calculated from the bubble size distribution Equation 10(c). At the lower boundary of the coalescence zone ($z = 0$) it is assumed that bubbles of identical

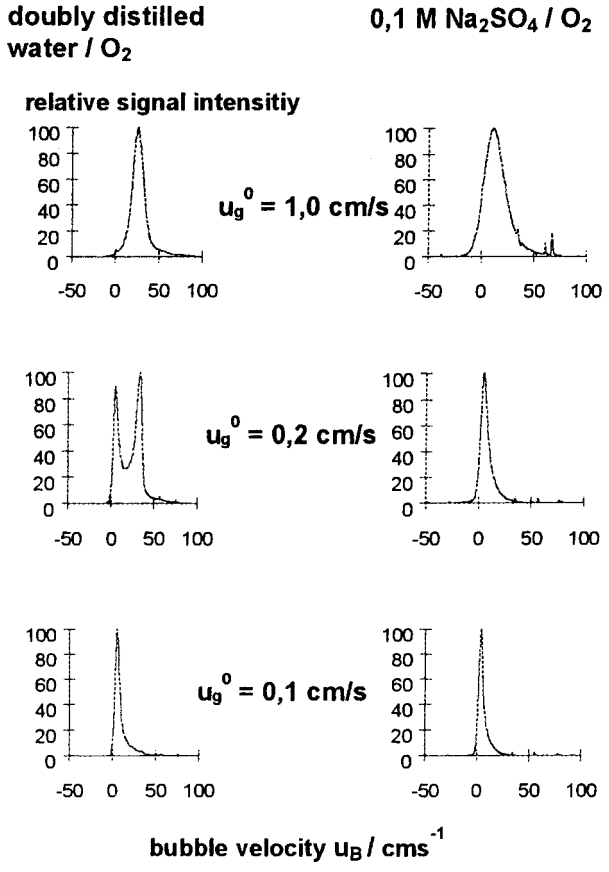

Fig. 10. Normalized bubble rise velocity distributions of O_2 in H_2O and 0.1 M Na_2SO_4 solution at different superficial gas velocities u_g^0.

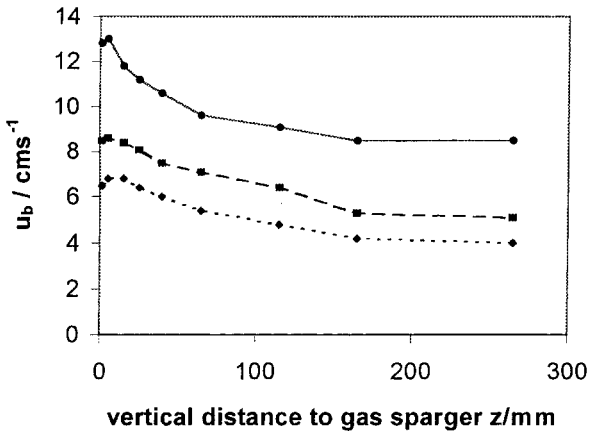

Fig. 12. Ultrasonic measurements of the axial profile of the bubble rise velocity, u_b, system: 0.1 M Na_2SO_4/O_2 at different superficial gas velocities u_g^0: 0.6 cm s^{-1} (●); 0.2 cm s^{-1} (■); 0.1 cm s^{-1} (◆).

diameter $d_{b,1}$ with rise velocity $u_{s,1}$ are formed at a concentration $c_{b,1}$ which depends on the gas flow rate u_g^0. A certain number of bubble classes, each characterized by a distinct value of the diameter, $d_{b,i}$, the rise velocity, $u_{s,i}$, and the concentration, $c_{b,i}$, is defined within the coalescence region $(0 < z < 1)$. The concentrations, $c_{b,i}$, are balanced by birth and death functions describing the disappearance and emergence of bubbles due to coalescence:

$$\text{For } z = 0: \quad d_{b,1},\ u_{s,1},\ c_{b,1}$$

$$0 < z < 1: \quad d_{b,i},\ u_{s,i},\ c_{b,i}$$

$$r_h = k\ \exp\left[\left(\frac{d_{b,i} \times d_{b,j}}{2d_{b,i}(d_{b,i} + d_{b,j})}\right)^{1.5}\right] \times \frac{v_c\left(1 - \frac{z}{l}\right)}{v_c\sqrt{\left(2 - \frac{z}{l}\right)\frac{z}{l}} + (u_{s,i} + u_{s,j})/2}(d_i + d_j)c_{b,i}c_{b,j} \quad (10a)$$

$$\frac{dc_{b,i}}{dz} = \sum_{\text{producing species i}} r_h - \sum_{\text{consuming species i}} r_h \quad (10b)$$

For $z = 1$:

$$\bar{d}_b = \frac{\sum c_{b,i}d_{b,i}}{\sum c_{b,i}}, \quad \bar{u}_s = \frac{\sum c_{b,i}u_{s,i}}{\sum c_{b,i}} \quad (10c)$$

where v_c is the velocity of a circulation flow observed above the gas sparger. This velocity can be calculated using an equation by Zehner [9, 16]. In Equation 10(b) the expression $k\ \exp[(d_{b,i} \times d_{b,j}/2d_{b,i}(d_{b,i} + d_{b,j}))^{1.5}]$ gives the probability of coalescence for bubbles, which are already in contact, where $\exp[(d_{b,i} \times d_{b,j}/2d_{b,i}(d_{b,i} + d_{b,j}))^{1.5}]$ is the term which represents the dependence of coalescence probability on the size [13, 22] and k is a system specific parameter, which depends on electrolyte concentration etc. The fraction

$$\frac{v_c\left(1 - \frac{z}{l}\right)}{v_c\sqrt{\left(2 - \frac{z}{l}\right)\frac{z}{l}} + (u_{s,i} + u_{s,j})/2}$$

is the ratio of the velocity that drives the bubbles towards the centre of the bubble column to the total rising velocity of the bubbles in the zone of circulation flow. $(d_i + d_j)c_{b,i}c_{b,j}$ is the probability that two bubbles with diameters d_i and d_j will collide at a certain level of z (note that the bubbles are not small compared to the length of the integration step; the concentrations of bubbles per volume are also assumed to represent the concentration of bubbles per unit area).

The bubble size distribution is computed by the following procedure. The initial bubble size $d_{b,1}$ at $z = 0$, that is, the bubble size that would prevail if no coalescence occurred, can be estimated by comparing calculated rise velocities of bubbles having a fixed diameter with measured bubble rise velocities at concentrations $c > 0.1$ M (e.g., in Fig. 5; $d_{b,1} = 0.24$ mm). The concentration of bubbles $c_{b,1}$ with diameter $d_{b,1}$ results from

$$c_{b,1} = \frac{u_g^0 A_{bc}}{u_{s,1}\frac{\pi}{6}d_{b,1}^3 A_{gs}} \quad (11)$$

Table 2. Balance of bubble volumes for a coalescence event

Educts *i, j*	*Product* *k*	*Reaction* *h*	$-\nu_{ih}, -\nu_{jh}$	ν_{kh}
1, –	2	1	2, –	1
1, 2	3	2	1, 1	1
1, $N/2$	$N/2 + 1$	$N/2$	1, 1	1
2, –	4	$N/2 + 1$	2, –	1
$N/2$, –	N	$N/2$ $(N/2+1)/2$	2, –	1

When bubbles coalesce the bubble volume will change in terms of $\pi d_{b,1}^3/6$. A classification of bubbles with diameter $d_{b,i}$ according to

$$d_{b,i} = \sqrt[3]{i}\, d_{b,1} \quad (12)$$

is introduced.

The change in the bubble volumes due to coalescence is given in Table 2. Coalescence is treated like a chemical reaction and therefore the volume of the bubbles is balanced similar to the elements in chemical reactions by using 'stoichiometric factors' ν_{ih}, ν_{jh} and ν_{kh}, so that the total volume of all bubbles remains constant. The indices i, j, k in Table 2 indicate the size of the bubbles involved in the coalescence process according to Equation 12. The index h is simply a counter which denotes a certain reaction rate r_h for the coalescence between two bubbles with diameters $d_{b,i}$ and $d_{b,j}$.

The parameter k in Equation 10(b) gives information about the probability of a successful coalescence event. Integration of the set of differential equations (Equation 10(b)) with the corresponding initial conditions Equations 11 and 12 up to the upper boundary $(z = 1)$ using a suitable algorithm [38], yields the final distribution and the mean values $\bar{d}_b$ and $\bar{u}_s$ as input parameters for the Nicklin equation (Equation 9). It should be pointed out that this model is restricted to lower gas input rates $u_g^0 < 4\,\text{cm s}^{-1}$ where the effects of turbulent flow on the ascent of bubbles above the coalescence zone can be neglected. Figure 13 shows optimum fit results for the gas hold-up of oxygen in

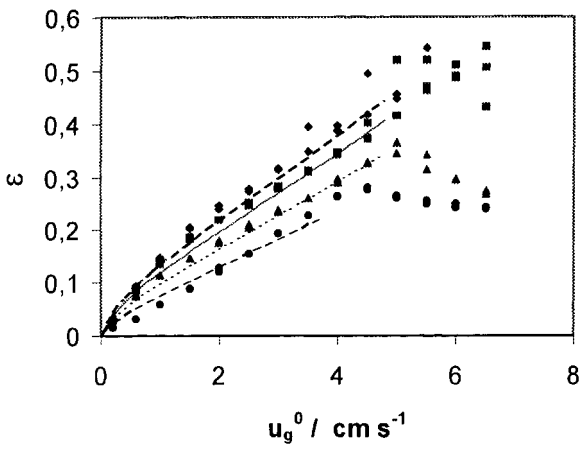

Fig. 13. Optimum fits of the coalescence zone model; systems: x M Na_2SO_4/O_2 $x = 0.3$ (◆), 0.2 (■), 0.1 (▲), 0.04 (●); fit parameter $k/10^5$ m 6.85 (— — —), 9.34 (—), 17.56 (- - -), 43.00 (– - -); fixed model parameters: $d_b = 0.24$ mm, $u_l^0 = 0.0$, $z = l = 10$ mm.

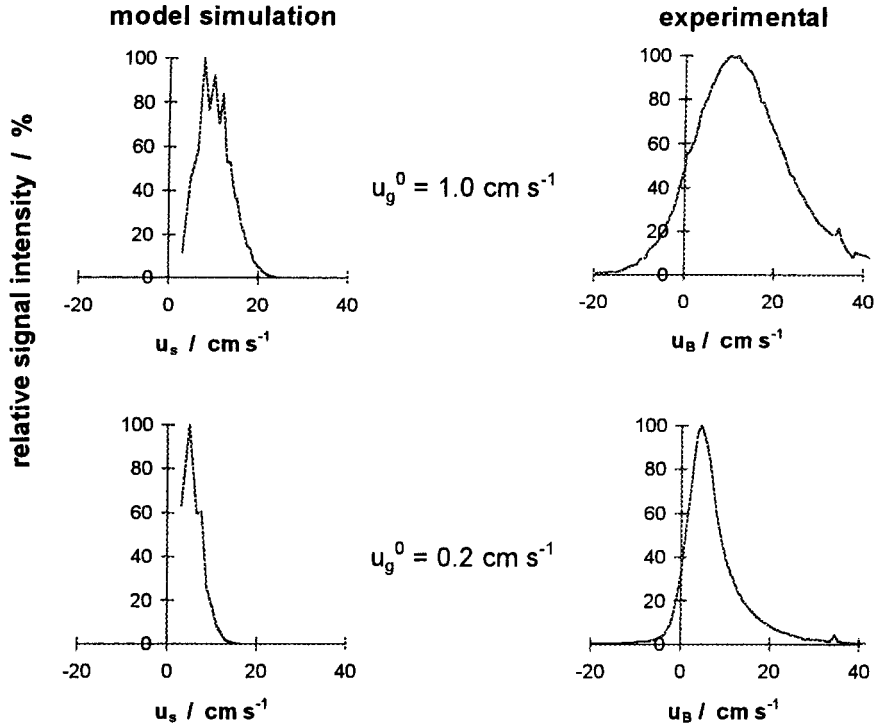

Fig. 14. Normalized bubble rise velocity distributions of O_2 in 0.1 M Na_2SO_4 solution, comparison of model simulation and experiment at different u_g^0.

Na_2SO_4 solutions of different concentrations. The curves calculated were obtained by adjusting the impact parameter k as the only fit parameter. The experimental values of the gas hold-up are well described up to a certain value of u_g^0, beyond which the model assumptions are no longer valid. As an additional result of the simulation, the distributions of the bubble rise velocities are also available as a function of u_g^0. Figure 14 shows experimental and computed distributions for two different u_g^0 values. Evidently, the trend of the real system is also well represented by the coalescence zone model. The broader distribution of the real system may be attributed to the existence of turbulent backflow.

The dependence of the impact parameter k, obtained from optimum fits in the system Na_2SO_4/O_2 and K_2SO_4/O_2, on the electrolyte concentration c is shown in Fig. 15. In both systems the probability of coalescence decreases with increasing electrolyte concentration. This reflects the impediment of coalescence, presumably due to surface tension differences on the surface of coalescing bubbles. The steep descent with low electrolyte concentrations is in accordance with the results of single bubble coalescence experiments reported by Marrucci and Nicodemo [19], Lessard and Zieminski [21] and Drogaris [22].

5. Conclusions

The gas hold-up measurements of oxygen and hydrogen in different elelctrolyte solutions show a significant dependence on the type and concentration of the electrolyte. In general the gas hold-up increases with increasing concentration. In all systems a maximum for the gas hold-up is attained at higher

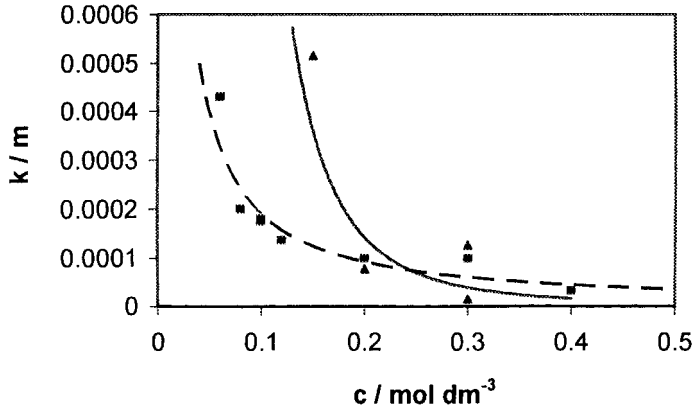

Fig. 15. Concentration dependence of the impact parameter k obtained from optimum fits of the experimental data of the gas hold-up ε of O_2 in Na_2SO_4 (■) and K_2SO_4 (▲) solutions.

superficial gas velocities u_g^0. In this paper it is shown for the first time that this maximum gas hold-up, ε_{max}, depends linearly on the ionic strength, I, of the solution, pointing to repulsive electrostatic interaction between the gas bubbles. However, the Debye length is as low as 1 nm in a 0.1 M solution of a 1–1-electrolyte like NaCl, whereas the thickness of rupturing films is a few 10 nm [20, 39]. Hence, electrostatic forces and the existence of an electric double layer cannot explain the dependence of the maximum gas hold-up on the ionic strength. The measurement of the bubble rise velocity distribution by an ultrasonic technique shows a distinct dependence on the gas flow rate, u_g^0, as a clear indication for the coalescence of bubbles. In the conventional models the coalescence of bubbles is not taken into account. Therefore, a new model, which considers coalescence events, was developed. This model is suitable to describe the experimental data in the homogeneous bubble flow regime in different electrolyte solutions by adjusting only one parameter, the coalescence impact parameter k. This parameter can be used to analyse the coalescence behaviour in electrolyte solutions with respect to theoretical considerations of the dynamics of the coalescence process.

Acknowledgement

The authors wish to acknowledge the financial support of this work by the Deutsche Forschungsgemeinschaft DFG, project Kv 615/7-1; Ju 201/3-2.

References

[1] E. Meredith and C. W. Tobias, *J. Electrochem. Soc.* **108** (1961) 286.
[2] L. Sigrist, O. Dossenbach and N. Ibl, *J. Appl. Electrochem.* **10** (1980) 223.
[3] G. Kreysa and M. Kuhn, *ibid.* **15** (1985) 517.
[4] M. Kuhn and G. Kreysa, *ibid.* **19** (1989) 720.
[5] M. Kuhn, Untersuchungen zum Einfluß des Gasgehaltes und der Elektrodengeometrie auf den Widerstand gasentwickelnder Elektrolysezellen, PhD thesis, University of Dortmund (1988).
[6] D. J. Nicklin, *Chem. Engng Sci.* **17** (1962) 693.
[7] J. F. Davidson and D. Harrison, *ibid.* **21** (1966) 731.
[8] M. J. Lockett and R. D. Kirkpatrick, *Trans. IChemE* **53** (1975) 267.
[9] P. Zehner, *Vt. Verfahrenstechnik* **16** (1982) 347.
[10] K. Akita, *Int. Chem. Eng.* **29** (1989) 127.
[11] M. Jamialahmadi and H. Müller-Steinhagen, *Chem.-Ing.-Techn.* **61** (1989) 715.
[12] M. Jamialahmadi and H. Müller-Steinhagen, *Trans. IChemE* **68** (1990) 202.
[13] M. J. Prince and H. W. Blanch, *AIChE J.* **36** (1990) 1425.
[14] J. Grienberger, Untersuchung und Modellierung von Blasensäulen, PhD thesis, Universität Erlangen, Nürnberg (1992).
[15] J. Zahradnik, M. Fialova, F. Kastanek, K. D. Green and N. H. Thomas, *Trans. IChemE* **73** (1995) 341.
[16] H. Kellermann, Untersuchungen zum Gas-Holdup von H_2 und O_2 in wäßrigen Elektrolytlösungen, PhD thesis, in preparation.
[17] H. Kellermann, K. Jüttner and G. Kreysa, *Chem. Techn.* **48** (1996) 156.
[18] *Idem*, *ibid.* **48** (1996) 16
[19] G. Marrucci and L. Nicodemo, *Chem. Engng Sci.* **22** (1967) 1257.
[20] G. Marrucci, *ibid.* **24** (1969) 975.
[21] R. R. Lessard and S. A. Zieminski, *Ind. Engng Chem. Fundam.* **10** (1971) 260.
[22] G. Drogaris and P. Weiland, *Chem. Engng Commun.* **23** (1983) 11.
[23] M. J. Prince and H. W. Blanch, *AIChE J.* **36** (1990) 1485.
[24] G. Keitel and U. Onken, *Chem. Engng Sci.* **37** (1982) 1635.
[25] Y. Fukui and S. Yuu, *AIChE J.* **28** (1982) 866.
[26] N. P. Brandon, G. H. Kelsall, S. Levine and A. L. Smith, *J. Appl. Electrochem.* **15** (1985) 485.
[27] G. H. Kelsall, S. Tang, S. Yurdakul and A. L. Smith, *J. Chem. Soc. Faraday Trans.* **92** (1996) 3887.
[28] G. Marrucci, *Ind. Engng Chem. Fundam.* **4** (1965) 224.
[29] G. Grund, A. Schumpe and W. D. Deckwer, *Chem. Engng Sci.* **47** (1992) 3509.
[30] B. Genenger and B. Lohrengel, *Chem. Engng Process.* **31** (1992) 87.
[31] S. A. Shetty, M. V. Kantak and B. G. Kelkar, *AIChE J.* **38** (1992) 1013.
[32] G. Kuncová and J. Zahradník, *Chem. Engng Process.* **34** (1995) 25.
[33] Th. Korte, Meßtechniken zur Charakterisierung von Blasensäulenreaktoren, das Ultraschallimpuls–Doppler–Anemometer, PhD thesis, University of Hanover (1986).
[34] B. P. Yao, C. Zheng, H. E. Gasche and H. Hofmann, *Chem. Engng Process.* **29** (1991) 65.
[35] H. F. Svendson, H. A. Jakobsen and R. Torvik, *Chem. Engng Sci.* **47** (1992) 3297.
[36] L. J. J. Janssen and E. Barendrecht, *Electrochim. Acta* **30** (1985) 683.
[37] M. Jamialahmadi, C. Branch and H. Müller-Steinhagen, *Trans. Inst. Chem. Eng.* **72** (1994) 119.
[38] W. H. Press, S. A. Teukolsky, W. T. Vetterling, B. P. Flannery, Numerical recipes in C, 2nd edn, Cambridge University Press, Cambridge (1992), p. 735
[39] R. D. Kirkpatrick and M. J. Lockett, *Chem. Engng Sci.* **29** (1974) 2363.